Communication

Broadband Decoupling Network for Dual-Band Microstrip Patch Antennas

Bai Cao Pan and Tie Jun Cui

***Abstract*— Microstrip antenna (MSA) has become one of the most popular techniques in the modern communication systems because of its potentials in diversities of operating band and polarization. With the development of highly compact circuits, the isolation between each terminal of a multi-input-multi-output (MIMO) system becomes more and more important to reach high system accuracy. Here, we propose an innovative approach of decoupling for a dual-band MSA, in which the isolation is achieved through two kinds of transmission lines based on the substrate integrated waveguide (SIW) and miniaturized spoof surface plasmon polariton (SSPP). Both SIW and SSPP transmission lines have been used in functional devices and could be considered as part of radio frequency front-end circuits. Using the proposed method, the isolation between two ports of MSA is achieved without occupying extra space. A prototype is fabricated on the basis of a triple-layer dual-band MSA, each port of which is connected to one of the novel transmission lines. Combining the perfectly high-pass SIW and low-pass SSPP, the proposed feeding network could provide broadband decoupling without influencing the property of the antenna. We show that the mutual coupling between two ports is decreased by almost 20 dB within a wide frequency band. Such a design could meet the needs in application of multiantenna or tunable system without further alteration in dimensions and has potential to play an important role in the future communication systems.**

***Index Terms*— Decoupling, dual band, spoof surface plasmon polaritons (SSPPs), substrate integrated waveguide (SIW).**

I. Introduction

Wireless network and communication, providing convenient and flexible services as mobile terminal, have witnessed tremendous growth in the past decades in both business and military fields. The increasing services diversification and system complexity lead to growing requirement for channel capacity and link reliability, as well as circuit integration, ease of fabrication and low costs. Multiband antennas with polarization diversity have been one of the most active embranchments of wireless technology to meet these requirement by covering more operating-band and providing dual-polarized (DP) or circularly polarized (CP) radiation with miniaturized sizes [1]. DP patch antennas have been widely used to combat multipath fading and improve the communication quality. They contribute to reduce the overall space of transmit/receive arrays and improve channel capacity and system stability. The DB antenna with multiple feed has become one of the most commonly used techniques in the multiple-input-multiple-output (MIMO) system.

To improve the stability of MIMO system, crosstalk between each component needs to be restrained, which give a requirement to reduce mutual coupling between each port of antennas. A variety of research focused on isolation improvement between different ports of dual-band patch antennas as well as signal leakage restraining between elements in arrays have been proposed, using electromagnetic band-gap structures [3], defected ground structure [4], lumped elements [5], decoupling network [6], and resonant metamaterial particles [7]–[9].

Up to now, most of the isolated designs consist of either decoupling arrays surrounding antennas or specific networks integrated at feeding terminals. The former situation leads to increasing difficulty in miniaturization. While the latter one would have impact on radiation property, which results in increased complexity in antenna design. Moreover, with the development of the tunable or controllable technology, it is important for the decoupling component to be adjustable and available in wide frequency range.

An interesting solution for decoupling in dual-band microstrip antenna (MSA) is to achieve signal isolation during transmission in radio frequency (RF) front-end circuits. By introducing the high-pass substrate integrated waveguide (SIW) [10]–[12] and low-pass spoof surface plasmon polaritons (SSPPs) [13]–[15] as excitations, two inputs can be highly isolated without more specific requirements for the antenna design. To emphasize advantages of such design, each novel feeding line provide high-pass or low-pass isolation while being part of some kinds of functional devices, such as power dividers and filters [11], [12], [14]. Moreover, the width of SSPP transmission line could be reduced by 70% by introducing interdigital structure (IS). The actual occupied space is small. In this communication, a plasmonic feeding network is presented, combining both SIW and SSPP transmission lines, each of which connects to one of the two orthogonal ports of a dual-band DP MSA. Owing to the research in the literature, such feeding network could be designed as a part of functional components in RF front-end circuits. The radiation property of the patch with and without the feeding network keeps stable. And the isolation between two ports within whole frequency band is improved by almost 20 dB.

II. Decoupling Network Design

The MSA could be excited either directly by coaxial probe or microstrip line, or indirectly coupling from microstrip lines, apertures, and coplanar waveguides. A traditional triple-layer dual-band MSA is shown in Fig. 1(a). The MSA consist of two media substrates, two orthogonal microstrip lines as feeds and a decorated rectangular patch. A quarter of the upper substrate is hidden from the view to give a better sight of the feeding lines. Since the area of metallic background would influence the radiation pattern of the antenna, certain free space needs to be considered for circuit design during analysis. Hence, the bottom substrate is extended by an area of 60 mm $\times$ 120 mm. Side view and top view of the triple-layer patch antenna are enlarged in Fig. 1(b) and (c). Two microstrip lines with impedance matching are set beneath the radiation patch separated by a media substrate, exciting the patch through electromagnetic coupling. The thicknesses of the substrates are 1 mm (lower substrate) and 0.8 mm (upper substrate), respectively. Both substrates are chosen to be F4B with relative permittivity of 2.65 and loss tangent of 0.002.

Manuscript received January 8, 2017; revised June 7, 2017; accepted July 26, 2017. Date of publication August 21, 2017; date of current version October 5, 2017. This work was supported by the National Science Foundation of China under Grant 61631007 and Grant 61571117. *(Corresponding author: Bai Cao Pan.)*

The authors are with State Key Laboratory of Millimeter Waves, School of Information Science and Engineering, Southeast University, Nanjing 210096, China, and also with the Synergetic Innovation Center of Wireless Communication Technology, Southeast University, Nanjing 210096, China (e-mail: panbaicaofly@163.com; tjcui@seu.edu.cn).

Color versions of one or more of the figures in this communication are available online at http://ieeexplore.ieee.org.

Digital Object Identifier 10.1109/TAP.2017.2742539

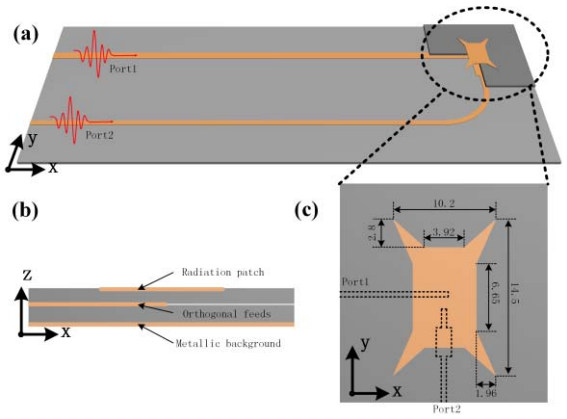

Fig. 1. (a) Schematic of the MSA with bottom substrate extended. A quarter of the upper substrate is hidden from view. (b) Side view and (c) top view of the MSA.

The detailed dimensions of the corner-tapered rectangular patch are labeled in Fig. 1(c). Four trapezoids are cut from each edge of a rectangular plate. The dashed outlines represent the location of the orthogonal feeds on the middle layer. The linewidth of the feeding lines at ports 1 and 2 are 2.74 and 1.6 mm, respectively. Each of them is responsible for a linear-polarized radiation on a corresponding frequency that is decided by dimensions of the patch. Port 1 excites the patch at a higher frequency since the patch is shorter along x-direction, while port 2 excites a radiation at a lower frequency. For the convenient of comparison, port 2 is guide into x-direction via a quarter-circle microstrip line. And both ports are extended to the edge of the substrate, as is shown in Fig. 1(a).

Since two feeding line is close to each other inside the antenna, signal would be coupled from one to the other while radiation or reflection. SIW and SSPP transmission lines are introduced to replace the microstrip lines as excitations. A sketch of the proposed decoupling network is shown in Fig. 2(a). An SIW waveguide is planted in the feeding line at port 1 to excite radiation at higher frequency and isolate signal leakage at lower frequencies. While an SSPP transmission line, providing low-pass filtering effect, connects port 2 and the antenna.

An SIW structure usually contains two row of via arrays as metallic walls and two transition parts at both terminals. As is fully discussed in literatures, SIW structures could support loss-less transmission with property similar to metallic rectangular waveguides. Signal at frequencies below the cutoff frequency would be filtered naturally. The detailed structure of the SIW is shown in Fig. 2(b). The cutoff property is directly decided by the separation of two metallic via rows, W_{SIW}. The relationship between width of SIW (W_{SIW}) and metallic rectangular waveguide (α) has already been obtained through the analytical MoM [10]

$$W_{\mathrm{SIW}} = \frac{2\alpha}{\pi} \arctan\left(\frac{\pi D}{4\alpha} \ln \frac{D}{4R}\right) \tag{1}$$

where R and D are the radius and cycle of vias, respectively. The SIW is connected with microstrip line through a 10 mm transition part with the linewidth narrowing from 10 to 2.74 mm which is required for 50 Ω impedance matching.

On the other hand, highly efficient excitation and transmission of the SSPP mode have already been studied on both single-strip and double-strip corrugated transmission line [14]. The structure of a miniaturized SSPP transmission line is shown in Fig. 2(c). Four ISs are introduced inside the grooves to provide lower cutoff properties. The comparison of dispersion relations of traditional and miniaturized

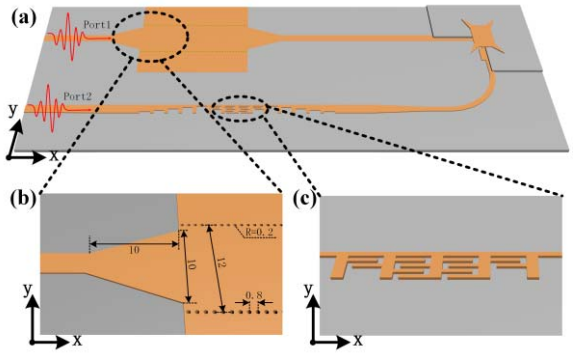

Fig. 2. (a) Schematic of the MSA with proposed decoupling feeding network. Detailed structures of (b) SIW and (c) miniaturized SSPP transmission lines.

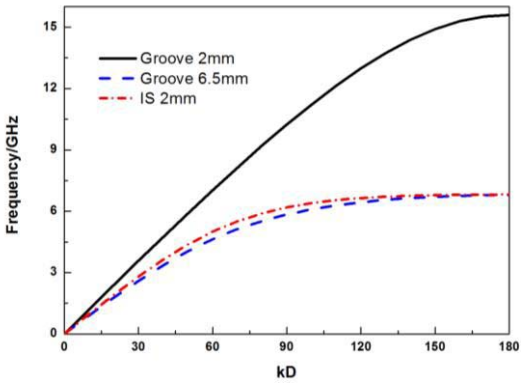

Fig. 3. Dispersion relations of traditional SSPP with grooves of 2 mm (black line) and 6.5 mm (dashed blue line) and miniaturized SSPP with groove of 2 mm (dashed-dotted red line).

SSPP is shown in Fig. 3. When depth of grooves is set to be 2 mm, the cutoff frequencies appear at 15.6 and 6.8 GHz for two cases, respectively. And when cutoff property of traditional SSPP is reduced to 6.8 GHz, the dimension increases to 6.5 mm. Compared with traditional SSPP, the width of the miniaturized SSPP structure is reduced by 70%.

III. Results and Discussion

Both models mentioned in Figs. 1 and 2 are simulated in the commercial software, CST Microwave Studio. In this prototype, the operating frequencies of MSA are designed at 6.4 and 8.2 GHz. The SIW and SSPP transmission lines are designed for transmission above and below 7.5 GHz, respectively. Such design could be available for most two-terminal networks or arrays with different operating bands. In practical application, the radiation frequencies could cover more frequency bands, such as WiMAX and WLAN applications. And the radiation components could be replaced without redesigning decoupling devices.

The simulated and measured reflections are shown in Fig. 4. The black line and dashed blue line represent simulated reflections at two ports of the MSA. Each port is responsible for one radiation at certain frequency. While the green line with dots and orange line with triangles are simulated reflections of MSA with the proposed feeding network. The bandwidth at higher frequency is narrowed when the feeding network is added. Such unfavorable fact can be eliminated by enlarging the space between an SIW and the patch. And several undesired resonant peaks appear because of the leaky wave of the SSPP structure. It can be avoided through further modifying of its coupling efficiency.

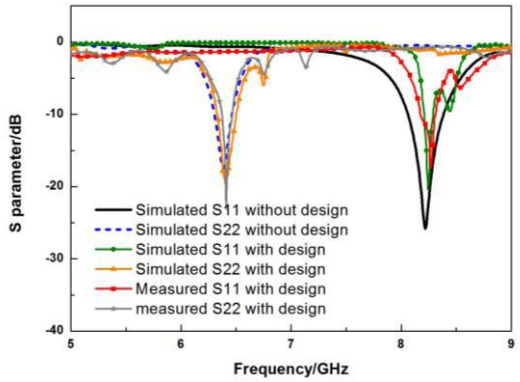

Fig. 4. Simulated and measured return losses of MSAs with and without the proposed decoupling feeding network.

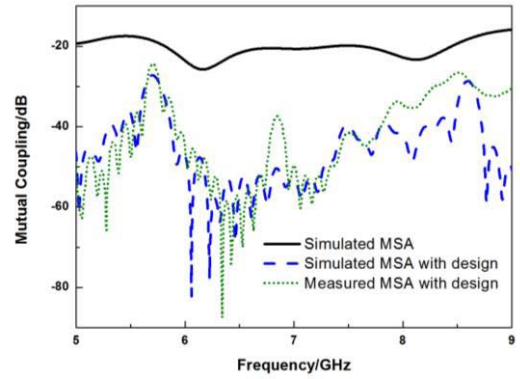

Fig. 5. Mutual coupling between two ports of the MSA with and without the proposed decoupling feeding network.

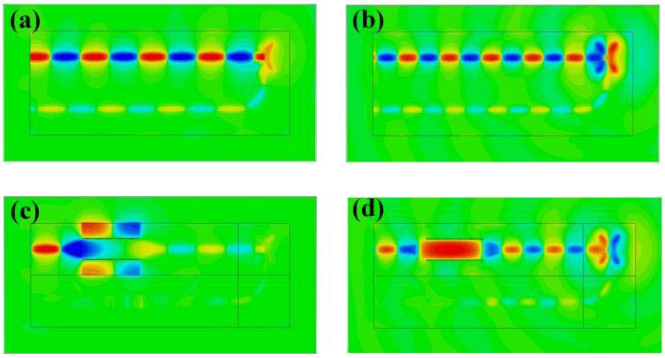

Fig. 6. Near electric field distribution of the circuits excited from port 1. Original MSA at (a) 6.4 GHz and (b) 8.2 GHz. MSA with the proposed decoupling feeding network at (c) 6.4 GHz and (d) 8.2 GHz.

The design is also measured through vector network. In the experiment, two subminiature version A connectors are used to connect the sample with coaxial lines. The red line with blocks and gray line with stars are measured results of the proposed design. Although a slightly shift of 40 MHz appears, the measured results agree with simulations well.

For the mutual coupling between two ports, since the network is reciprocal, only S21 is compared. As is shown in Fig. 5, the black line shows the transmission coefficient from port 1 to port 2. The blue dashed line and green dotted line are the simulation and measured results of MSA with the proposed design. It is clear to see that the isolation between two ports is significantly improved by about 20 dB within the whole band. And machining error and

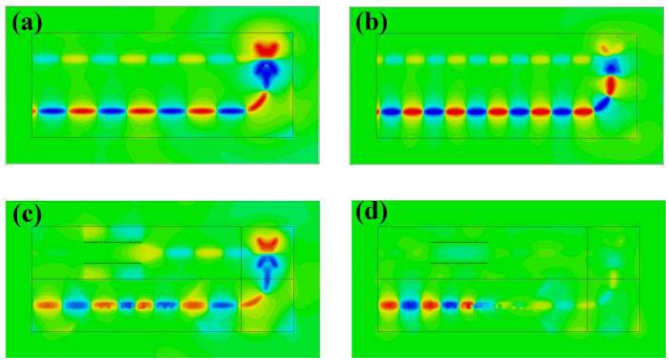

Fig. 7. Near electric field distribution of the circuits excited from port 2. Original MSA at (a) 6.4 GHz and (b) 8.2 GHz. MSA with the proposed decoupling feeding network at (c) 6.4 GHz and (d) 8.2 GHz.

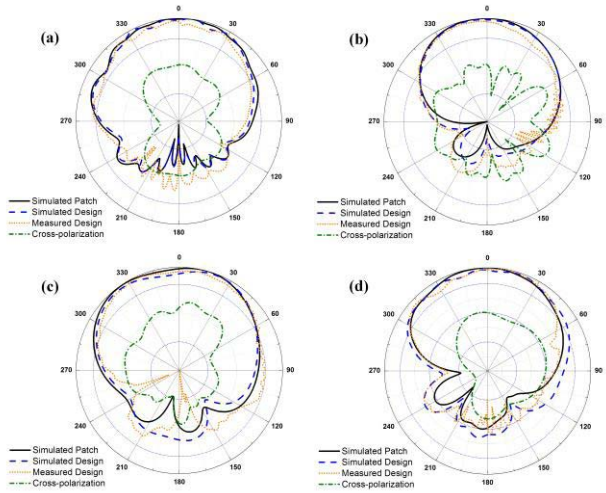

Fig. 8. (a) E-plane and (b) H-plane of the MSA with and without the proposed decoupling feeding network at 8.2 GHz. (c) E-plane and (d) H-plane of the MSA with and without the proposed decoupling feeding network at 6.4 GHz.

nonideal experimental environment may be the main reason of that the improvement of measured result is relatively weaker than that of simulation.

In order to give a more intuitive explanation of the decoupling mechanism, the electric field distribution inside the circuit is simulated. Since the field mainly exists inside SIW and SSPP transmission lines, the reference plane is chose to be an x-y-cut-plane in the middle of the bottom substrates. Figs. 6 and 7 illustrate the comparison of near-field distribution between the MSA with and without the decoupling design, excited from ports 1 and 2 at both operating frequencies, respectively. The signal from port 1 is reflected at the patch area in Fig. 6(a) and the patch is excited in Fig. 6(b). Certain level of signal leakage can be observed toward port 2 from the patch area in both cases. While when the decoupling design is added, the situation is improved. At 6.4 GHz, the signal from port 1 is directly reflected at the edge of SIW structures [Fig. 6(c)]. And at 8.2 GHz, the signal leakage would be cutoff by the SSPP structure [Fig. 6(d)]. On the other hand, signal from port 2 could excite the antenna at 6.4 GHz [Fig. 7(a)] and be reflected at 8.2 GHz [Fig. 7(b)]. In the decoupling design, the SIW is responsible for isolation of the leakage at 6.4 GHz [Fig. 7(c)]. And the SSPP isolates signal at higher frequency from the patch [Fig. 7(d)]. Through the comparison of near-field distribution, it is sure that the isolation is improved by the proposed design.

The normalized simulated and measured far-field radiation patterns are shown in Fig. 8. The black lines are simulated patterns of

the MSA in Fig. 1. And the dashed blue lines and the dotted orange lines are simulated and measured patterns of the proposed design in Fig. 2. E-plane and H-plane at 8.2 GHz are shown in Fig. 8(a) and (b). The half-power beamwidth (HPBW) of them are 75.2° and 76°, respectively. HPBWs of E-plane [see Fig. 8(c)] and H-plane [see Fig. 8(d)] at 6.4 GHz are 110.8° and 79.9°, respectively. The measurement agrees with the simulation well. The dashed-dotted green lines in Fig. 8 are radiation patterns of cross polarization at certain frequencies. There is almost 20 dB difference between the radiation patterns of two polarizations.

The total efficiencies of MAS at 6.4 and 8.2 GHz are 90.8% and 94.3%, respectively. And the total efficiencies of the design at 6.4 and 8.2 GHz are 90.9% and 86.7%. The efficiency of the design at port 2 is relatively lower because of the transmission loss during the transition part between SSPP and microstrip line. This could be restrained by lengthening the groove-depth-changing part from 5 to 8 units.

IV. Conclusion

In summary, we proposed a decoupling feeding network combining SIW and miniaturized SSPP transmission lines. The cutoff frequency of SSPP is supposed to be a little lower than that of SIW to ensure that no overlapped passband exists within the whole band. The SIW isolates signal leakage between port and antenna at lower frequency while SSPP is responsible for isolation at higher frequency. Such design is available for most dual-band or dual-broadband networks, and the radiation components could be changed without redesigning the decoupling network, as long as two operating bands are located at two sides of the cutoff frequency. Moreover, owing to the development of functional devices based on SIW and SSPP, such feeding network could work as part of the RF circuits. Namely, isolation is obtained in the RF front-end without occupying extra space or influencing the antenna. The measurement agrees well with simulations. Such designs have potentials to play an important role in the future plasmonic integrated circuits and systems.

References

[1] P. K. Mishra, D. R. Jahagirdar, and G. Kumar, "A review of broadband dual linearly polarized microstrip antenna designs with high isolation," *IEEE Antennas Propag. Mag.*, vol. 56, no. 6, pp. 238–251, Dec. 2014.

[2] G. Kumar and K. P. Ray, *Broadband Microstrip Antennas*. Norwood, MA, USA: Artech House, 2003, pp. 1–27.

[3] S. D. Assimonis, T. V. Yioultsis, and C. S. Antonopoulos, "Computational investigation and design of planar EBG structures for coupling reduction in antenna applications," *IEEE Trans. Magn.*, vol. 48, no. 2, pp. 771–774, Feb. 2012.

[4] A. Farahbakhsh, M. Mosalanejad, G. Moradi, and S. Mohanna, "Using polygonal defect in ground structure to reduce mutual coupling in microstrip array antenna," *J. Electromagn. Waves Appl.*, vol. 28, no. 2, pp. 194–201, 2014.

[5] C.-H. Wu, C.-L. Chiu, and T.-G. Ma, "Very compact fully lumped decoupling network for a coupled two-element array," *IEEE Antennas Wireless Propag. Lett.*, vol. 15, pp. 158–161, 2016.

[6] L. Zhao, L. K. Yeung, and K.-L. Wu, "A coupled resonator decoupling network for two-element compact antenna arrays in mobile terminals," *IEEE Trans. Antennas Propag.*, vol. 62, no. 5, pp. 2767–2776, May 2014.

[7] A. Habashi, J. Nourinia, and C. Ghobadi, "Mutual coupling reduction between very closely spaced patch antennas using low-profile folded split-ring resonators (FSRRs)," *IEEE Antennas Wireless Propag. Lett.*, vol. 10, pp. 862–865, 2011.

[8] X. M. Yang, X. G. Liu, X. Y. Zhou, and T. J. Cui, "Reduction of mutual coupling between closely packed patch antennas using waveguided metamaterials," *IEEE Antennas Wireless Propag. Lett.*, vol. 11, pp. 389–391, 2012.

[9] B. C. Pan, W. X. Tang, M. Q. Qi, H. F. Ma, Z. Tao, and T. J. Cui, "Reduction of the spatially mutual coupling between dual-polarized patch antennas using coupled metamaterial slabs," *Sci. Rep.*, vol. 6, p. 30288, Jul. 2016.

[10] W. Che, L. Xu, D. Wang, L. Geng, K. Deng, and Y. L. Chow, "Equivalence between substrate-integrated rectangular waveguide (SIRW) bend and rectangular waveguide (RW) bend," *Microw. Opt. Technol. Lett.*, vol. 48, no. 9, pp. 1694–1698, 2006.

[11] A. Sahu, V. K. Devabhaktuni, R. K. Mishra, and P. H. Aaen, "Recent advances in theory and applications of substrate-integrated waveguides: A review," *Int. J. RF Microw. Comput. Aided Eng.*, vol. 26, no. 2, pp. 129–145, 2016.

[12] D. S. Eom, J. Byun, and H. Y. Lee, "Multilayer substrate integrated waveguide four-way out-of-phase power divider," *IEEE Trans. Microw. Theory Techn.*, vol. 57, no. 12, pp. 3469–3476, Dec. 2009.

[13] B. C. Pan, H. C. Zhang, and T. J. Cui, "Multilayer transmissions of spoof surface plasmon polaritons for multifunctional applications," *Adv. Mater. Technol.*, vol. 2, no. 1, p. 1600159, 2017, doi: 10.1002/admt.201600159.

[14] L. Liu, Z. Li, B. Xu, J. Xu, C. Chen, and C. Gu, "Fishbone-like high-efficiency low-pass plasmonic filter based on double-layered conformal surface plasmons," *Plasmonics*, vol. 12, no. 2, pp. 439–444, 2017, doi: 10.1007/s11468-016-0283-5.

[15] Y. Wu, M. Li, G. Yan, L. Deng, Y. Liuand, and Z. Ghassemlooy, "Single-conductor co-planar quasi-symmetry unequal power divider based on spoof surface plasmon polaritons of bow-tie cells," *AIP Adv.*, vol. 6, no. 10, p. 105110, 2016.